STM and XPS Studies of the Oxidation of Aniline at Cu(110) Surfaces

Philip R. Davies,* Dyfan Edwards, and Darran Richards

School of Chemistry, Cardiff University, P.O. Box 912, Cardiff CF10 3TB, U.K.

Received: May 27, 2004; In Final Form: September 8, 2004

Aniline chemisorption at clean and partially oxidized Cu(110) surfaces at 293 K is compared with the reaction of a 300:1 aniline/dioxygen mixture at the same surface using STM and XPS. Limited dissociation occurs at the clean surface but in the presence of chemisorbed oxygen efficient oxy-dehydrogenation takes place with water desorption and the formation of chemisorbed phenyl imide ($C_6H_5N(a)$) with a reaction stoichiometry that changes with coverage. The adsorption site of the phenyl group is identified by STM to be the 2-fold hollow and it is proposed that the nitrogen is situated over the short bridge site. Chemisorptive replacement of oxygen gives a maximum phenyl imide concentration of 2.8×10^{14} molecules cm^{-2} at which coverage the surface is dominated by a mixture of three ordered domains with structures described by $\begin{pmatrix} 4 & 0 \\ 2 & 2 \end{pmatrix}$, $\begin{pmatrix} 4 & 0 \\ -1 & 2 \end{pmatrix}$, and $\begin{pmatrix} 4 & 0 \\ 1 & 2 \end{pmatrix}$ unit meshes. Adsorption of aniline and dioxygen mixtures however results in phenyl imide concentrations up to 3.4×10^{14} cm^{-2} molecules cm^{-2} and a highly ordered biphasic structure characterized by $\begin{pmatrix} 3 & 0 \\ -1 & 2 \end{pmatrix}$ and $\begin{pmatrix} 3 & 0 \\ 1 & 2 \end{pmatrix}$ domains. A discrepancy between the concentrations measured by XPS and those calculated from the STM structures is discussed in terms of π-stacking of the phenyl rings in the adsorbed monolayer. Finally the chemistry of aniline is compared with that of ammonia and the importance of the NH bond strength and the basicity of the amine discussed.

Introduction

Amines have applications in many interface related areas including corrosion inhibition,[1−5] adhesion,[6−10] and heterogeneous catalysis.[11,12] In the latter case, amines are commonly used not only as reactants but also as catalyst modifiers.[12−14] Pfaltz, for example, has shown[15] that a basic nitrogen group is a necessary component of chiral modifiers for the hydrogenation of α-functionalized ketones.[16−20] The interaction of the amine functionality with the surface is therefore a subject of some importance in surface science. Our own interest in amine surface chemistry stems from studies of ammonia oxidation[21−30] and of the interaction of pyridine with surface oxygen, where intermolecular complexes between pyridine and both molecular oxygen transients[31] and chemisorbed atomic oxygen[32,33] have been demonstrated. In this paper, we consider the reaction of aniline with oxygen at Cu(110) surfaces. Aniline has a lower basicity ($pK_b = 9.37$) than either ammonia ($pK_b = 4.75$) or pyridine ($pK_b = 8.75$), and the reaction with oxygen may also be sterically hindered by the phenyl ring.

Previous studies of aniline surface chemistry have concentrated on adsorption at clean metal[34−44] or clean silicon surfaces[45,46] using temperature-programmed desorption (TPD) and vibrational spectroscopy (HREELS). It has been reported[47] that the molecule dissociates at clean Cu(110) surfaces to give an amide (PhNH(a)) in which the phenyl ring lies approximately parallel to the surface but there have been no structural studies of the reaction.

Experimental Section

Experiments were conducted using a combined variable temperature STM/XPS instrument (Omicron Vacuum Physik) equipped with a dual Al Kα and Mg Kα photon source. Except where stated otherwise, XP spectra were recorded with a pass energy of 100 eV resulting in typical peak half-widths of ca. 2.0 eV. Spectra were obtained by the combination of 10−20 individual scans over a 25 eV wide region, with a total acquisition time of between 10 min (O(1s) and Cu (2p) spectra) to 20 min (C(1s) and N(1s) spectra). The spectra were calibrated to the clean $Cu(2p_{3/2})$ peak at 932.7 eV. XPS data was acquired using commercial software (Spectra, Ron Unwin) and analyzed using software developed in-house. Surface concentrations were calculated from XP peak areas using the method discussed previously.[48,49] We estimate the error in surface concentrations of oxygen to be $\pm 1.5 \times 10^{13}$ cm^{-2} and to be slightly greater in the case of carbon and nitrogen, which have weaker signals.

The dimensions of the sample were 7 mm by 7 mm with a thickness of approximately 0.5 mm, it was cut to within 0.5° of the (110) plane and polished mechanically down to 0.25 μm. Cleaning involved cycles of Ar^+ sputtering (0.75 keV, 20 μA cm^{-2} for 20 min) and annealing for 60 min at 900 K. This resulted in flat terraces approximately 10−20 nm wide in the STM images. Sample cleanliness was checked by XPS. Gases were dosed via a leak valve at pressures of between 10^{-9} and 5×10^{-7} mbar. The aniline (Aldrich, 99.5%) was subjected to several freeze pump thaw cycles using a dry ice/acetone slush and its purity was monitored with in-situ mass spectrometry. Oxygen (Argo Ltd, 99.998%) was used as received.

Results

3.1. XPS Investigations. *3.1.1. Aniline Adsorption at Clean and Preoxidized Cu(110) Surfaces*. In contrast to ammonia[28] and other amines[50] which do not react with clean copper surfaces, Figure 1a shows that exposure of a clean Cu(110)

* Corresponding author. E-mail: daviespr@cf.ac.uk.

10.1021/jp047697l CCC: $27.50
Published on Web 11/06/2004

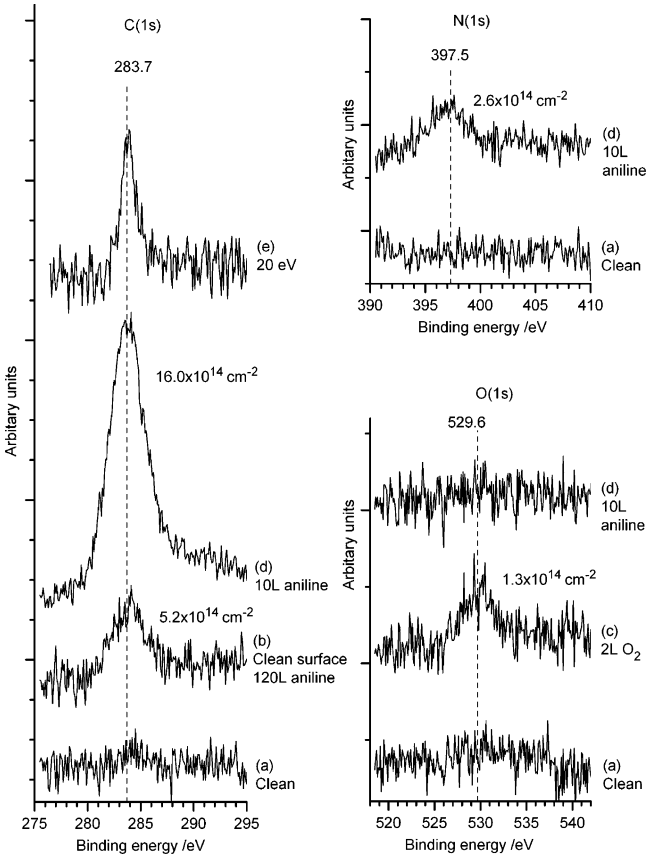

Figure 1. XP C(1s), N(1s), and O(1s) spectra comparing aniline adsorption at clean and partially oxidized Cu(110) surfaces at 293 K: (a) clean surface; (b) clean Cu(110) surface after exposure to 120 langmuir of aniline at 293 K; (c) clean surface after exposure to 2 langmuir of O_2(g); (d) surface in part c after exposure to 10 langmuir of aniline. (e) C(1s) spectrum of the surface in part d recorded at 20 eV pass energy to establish the presence of a single carbon state.

surface to aniline at 293 K leads to some adsorption with a single peak appearing in the XP C(1s) region at a binding energy of 283.7 eV, which reaches maximum intensity after ca. 120 L (1 langmuir = 10^{-6} Torr s)

The surface concentration of carbon, calculated from the XP peak area, is 5.2×10^{14} cm^{-2}. The corresponding N(1s) spectrum shows some intensity increase but the peak is too weak to calculate a reliable concentration.

More extensive adsorption results when aniline is dosed in the presence of preadsorbed oxygen. Figure 1c shows an XP O(1s) spectrum of a Cu(110) surface with an initial oxygen concentration of 1.3×10^{14} cm^{-2}. When this surface is exposed to 10 langmuir of aniline at 293 K, Figure 1d, a facile reaction occurs resulting in the desorption of all the oxygen, presumably as water,[28] and its replacement by a species containing carbon and nitrogen with binding energies of 283.7 and 397.5 eV respectively. The carbon:nitrogen ratio calculated from the XP peak areas is 6:1, and the nitrogen concentration (2.6×10^{14} cm^{-2}) is twice that of the initial oxygen concentration. Exposures up to 120 langmuir gave rise to no further adsorption. High resolution spectra of the C(1s) region, Figure 1e, show only a single carbon state at the surface and this can be assigned on the basis of the carbon/nitrogen ratio and the characteristically low binding energy to a phenyl group.[51,52] The N(1s) peak binding energy of 397.5 eV is characteristic of imide chemisorbed at copper surfaces, amides and nitrides typically giving rise to peak binding energies at 399 and 396.5 eV respectively.[28,29] These assignments are discussed in more detail below.

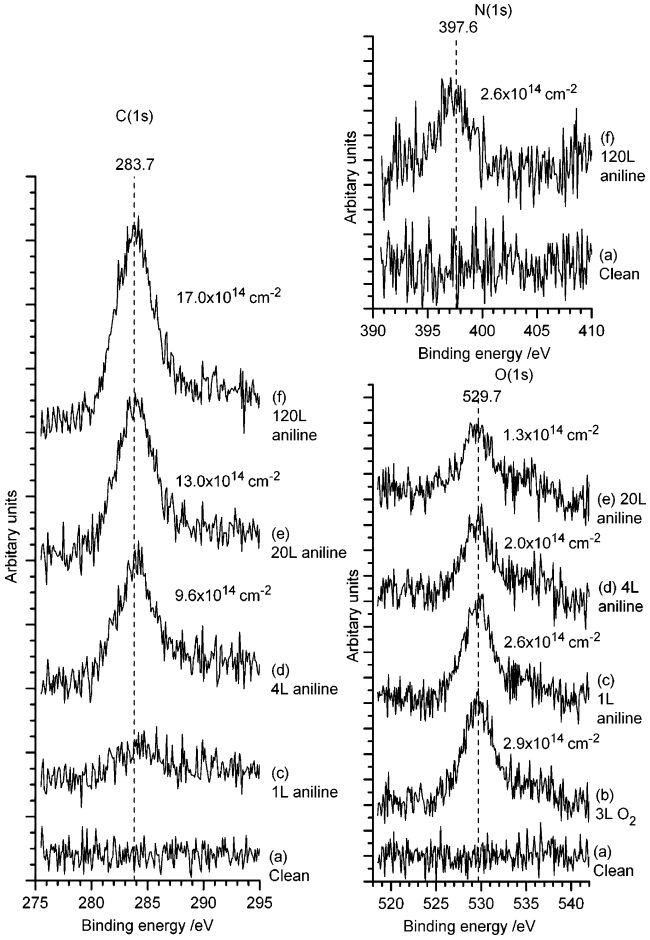

Figure 2. XP C(1s), N(1s), and O(1s) spectra of the chemisorption of aniline at 293 K at a Cu(110) surface with a higher initial oxygen concentration than that shown in Figure 1. Note the change in the ratio of phenyl groups added to oxygen removed from 2:1 after 4 langmuir of aniline to 1:1 after 120 langmuir: (a) clean surface; (b) surface after exposure to 3 langmuir of O_2(g); (c) surface after exposure to 1 langmuir of aniline; (c) surface after exposure to 4 langmuir of aniline; (d) surface after exposure to 8 langmuir of aniline; (e) surface after exposure to 20 langmuir of aniline; (f) surface after exposure to 120 langmuir of aniline.

For oxygen concentrations greater than ca. 2.5×10^{14} cm^{-2} but less than a monolayer (5.5×10^{14} cm^{-2}), reaction with aniline remains facile at room temperature with identical XP binding energies indicating that the reaction product is the same as that observed at lower oxygen concentrations. However, there is a marked change in stoichiometry as the reaction progresses. Figure 2 shows that for an oxygen concentration of 2.9×10^{14} cm^{-2}, exposure to aniline results, after 4 langmuir, in a 2:1 aniline:oxygen reaction stoichiometry (parts b and d), but this changes to 1:1 with a further exposure of 20 langmuir (parts d and e). For initial oxygen concentrations close to a monolayer, reaction is limited in extent at room temperature and the reaction stoichiometry is 1:1. A monolayer of preadsorbed oxygen completely inhibits aniline reaction for exposures up to 200 langmuir at room temperature.

3.1.2. Coadsorption of Aniline and Dioxygen at Clean Cu-(110) Surfaces. Figure 3 shows XP spectra obtained after the clean copper surface was exposed to 200 langmuir of a 300:1 aniline:oxygen mixture at 293 K. The total oxygen exposure is 0.7 langmuir but the XP data shows no oxygen at the surface. Instead, peaks in the C(1s) and N(1s) regions at binding energies of 283.8 and 397.8 eV indicate the presence of the same species observed after aniline reaction with *preadsorbed* oxygen. The

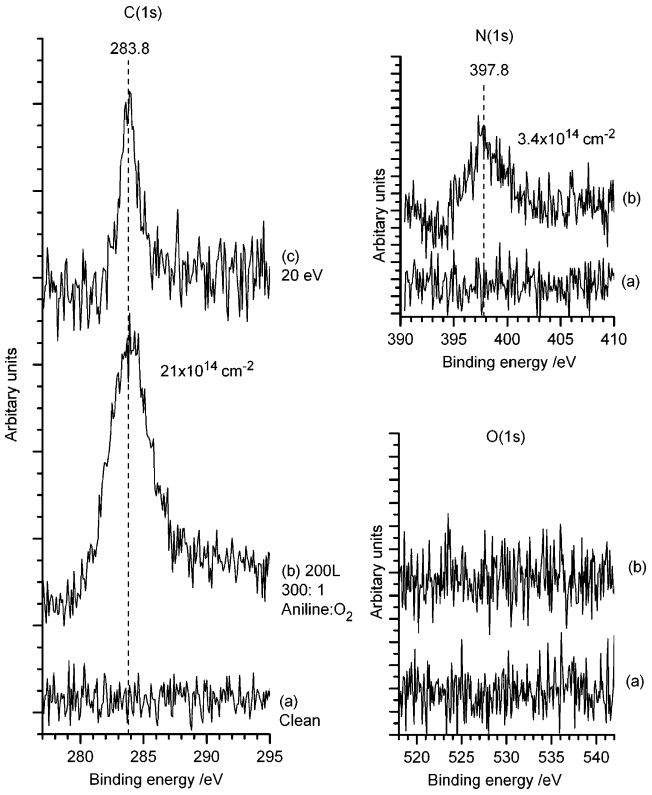

Figure 3. XP C(1s), N(1s), and O(1s) spectra of the adsorption of aniline and dioxygen at a Cu(110) surface in a 300:1 mixture at 293 K: (a) clean surface; (b) surface after exposure to 200 langmuir of mixture; (c) high resolution 20 eV pass energy spectrum of the surface in part b.

coadsorption of reactants results not only in an efficient reaction that converts all of the oxygen adsorbing at the surface but also in a higher concentration of the phenyl imide product than was obtained through sequential adsorption of the reactants, the final carbon concentration being 2.1×10^{15} cm^{-2}.

3.2. STM Investigations. *3.2.1. Aniline Adsorption at Clean and Preoxidized Cu(110) Surfaces.* No ordered adlayer structures were observed by STM for aniline reaction with the clean Cu(110) surface, and no reaction was evident in the STM images when a surface with a monolayer of oxygen present (5.5×10^{14} cm^{-2}) was exposed to aniline. At oxygen coverages below 5×10^{14} cm^{-2}, however, aniline adsorption is observed at step edges and at defect sites in the lattice; a typical image is shown in Figure 4a for an initial oxygen concentration of 4.8×10^{14} cm^{-2}. At lower oxygen concentrations the imide product from the aniline can be imaged simultaneously with the p(2 × 1)O(a) lattice. Figure 4b shows the characteristic p(2 × 1) oxygen islands surrounded by the phenyl imide product after a surface with an initial oxygen concentration of 2.4×10^{14} cm^{-2} was exposed to 20 langmuir of aniline at room temperature. The phenyl imide structure does not exhibit long range order, but some evidence for local structure is present, related to the unit cells described in more detail below. It is also clear from Figure 4b that aniline adsorption does not result in any expansion of the oxygen lattice in the $\langle 1\bar{1}0 \rangle$ direction as was observed in the case of pyridine[32] and some other amines.[50]

The majority of imide features appear 0.1 nm above the oxygen although some features 0.3 nm above are also observed, Figure 4, parts c and d. Extrapolating the oxygen (2 × 1) lattice over imide covered areas in Figure 4b establishes that, in both the $\langle 100 \rangle$ and $\langle 1\bar{1}0 \rangle$ directions, the imide features are in line with the maxima in the oxygen p(2 × 1) lattice.

Improved long range order in the phenyl imide adlayer was obtained when low oxygen coverages were completely removed by reaction with aniline. Images were obtained for carbon concentrations of around 1.6×10^{14} cm^{-2}, corresponding to an imide concentration of 2.7×10^{14} cm^{-2}, and in all cases had a characteristic "zigzag" appearance at low resolution; examples are shown in Figure 5. The zigzag appearance arises from ordered sets of lines which occur in domains generally 3−4 nm in length (though several extend to 9 nm) and 5−6 lines wide (approximately 5−6 nm although some involve more than 10 lines over approximately 10 nm.) The lines, are orientated either along the $\langle 1\bar{1}0 \rangle$ axis or at ±20 degrees to it. In the $\langle 100 \rangle$ direction, the spacing between the lines is 1.0 nm.

Individual molecular features are also observed in the STM images, examples are shown in Figure 6, parts a and b with a close up of the molecularly resolved features near to two step edges in Figure 6c. The adsorbed imides are approximately 0.7 nm in diameter with height corrugations between features of ∼0.05 nm. No details were resolved within these features. The imides are best imaged with a positive sample bias and closely resemble those observed[53,54] following the dissociative adsorption of phenyl iodide, they are assigned to the phenyl ring of the imide.

In Figure 7, parts a−c, molecularly resolved images of each of the three characteristic domains are shown. The unit cells for all three structures have in common a 1.0 nm vector in the $\langle 1\bar{1}0 \rangle$ direction corresponding to four times the substrate lattice and, as we discuss in more detail below, can be described in matrix notation[55] by $\begin{pmatrix} 4 & 0 \\ 2 & 2 \end{pmatrix}$, $\begin{pmatrix} 4 & 0 \\ -1 & 2 \end{pmatrix}$, and $\begin{pmatrix} 4 & 0 \\ 1 & 2 \end{pmatrix}$ unit cells.

Figure 8a shows an STM image obtained from a surface on which an oxygen concentration of 2.4×10^{14} cm^{-2} was exposed to 200 langmuir of aniline. Although molecular scale features can still be resolved after reaction, there is no long-range order and little evidence for short-range order except for a tendency for features to align in the $\langle 1\bar{1}0 \rangle$ direction.

3.2.2. Coadsorption of Aniline and Dioxygen at Clean Cu(110) Surfaces. Parts b and c of Figure 8 show STM images corresponding to the XP data in Figure 3 obtained after a clean Cu(110) surface was exposed to 200 langmuir of a 300:1 aniline/oxygen mixture at 293 K and which gave a final carbon concentration of 2.1×10^{15} cm^{-2}. There are two major differences between the image in Figure 8b and that in Figure 8c and those obtained when oxygen is preadsorbed. First, the surface is characterized by considerably shorter terraces than those of the clean surface, and the profile in Figure 8d shows that nearly all the steps at the surface are of single atomic dimensions (the interplane spacing for a Cu(110) surface being 0.13 nm) whereas at the clean and partially oxidized surfaces, steps are typically bunched in twos or threes. Second, a high degree of adsorbate ordering is present after coadsorption. The phenyl imide adlayer can be described with $\begin{pmatrix} 3 & 0 \\ -1 & 2 \end{pmatrix}$ and $\begin{pmatrix} 3 & 0 \\ 1 & 2 \end{pmatrix}$ unit meshes which are clearly related, by a compression in the $\langle 1\bar{1}0 \rangle$ direction, to the lower coverage $\begin{pmatrix} 4 & 0 \\ -1 & 2 \end{pmatrix}$ and $\begin{pmatrix} 4 & 0 \\ 1 & 2 \end{pmatrix}$ structures identified above.

4. Discussion

4.1. Identification of the Chemisorbed Reaction Product. We consider first the identity of the surface species resulting

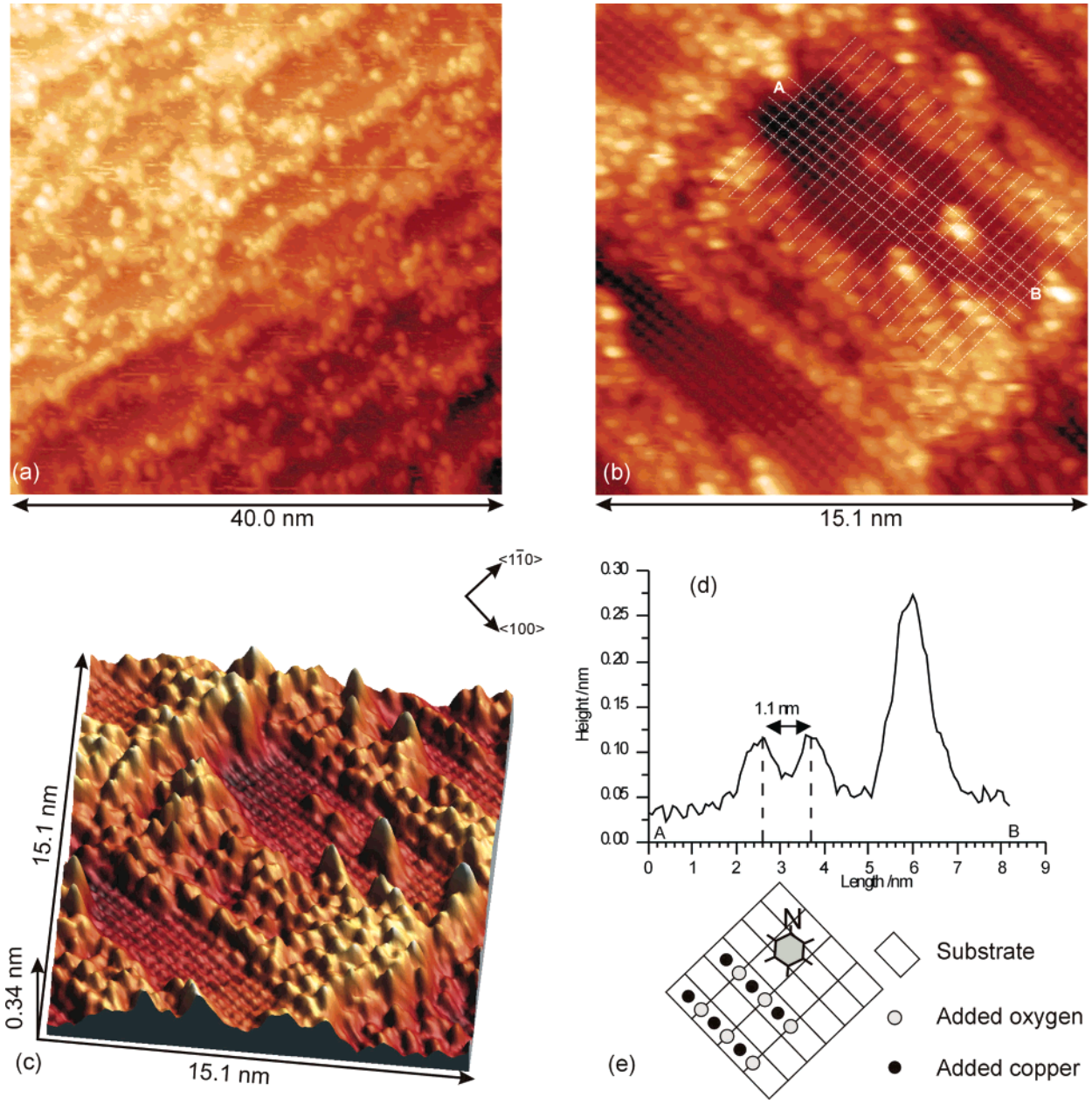

Figure 4. STM images recorded after the reaction of aniline with different concentrations of preadsorbed oxygen at a Cu(110) surface at 293 K: (a) initial oxygen concentration of 4.8×10^{14} cm^{-2} exposed to 20 langmuir of PhI at 293 K, $V_S = +1.22$ V, $I_T = 1.80$ nA; (b) initial oxygen concentration of 2.4×10^{14} cm^{-2} exposed to 20 langmuir of PhI at 293 K, $V_S = +1.07$ V, $I_T = 2.32$ nA. The grid superimposed on the image extrapolates the p(2 × 1)*O*(*a*) structure over the adsorbed imide. (c) 3d rendering of the topography from part b. (d) Line profile along AB in part b. (e) Model of proposed adsorption site of phenyl imide together with the p(2 × 1)O(a) lattice.

from the reaction of aniline with oxygen. The XP data indicates that the same species is formed under all the conditions studied here. The C(1s) binding energy of 293.7 eV and the 0.7 nm diameter features in the STM images agree well with previous studies[53,54] of phenyl groups at copper surfaces, and the consistent 6:1 C:N ratio with the N(1s) binding energy of 397.8 eV indicate that the C−N bond remains intact. The adsorbed species can therefore be assigned to either an amide (C_6H_5NH-(a)) or an imide (C_6H_5N(a)) with the latter being indicated by the N(1s) binding energy of 397.8 eV; amides giving N(1s) binding energies in the region of 399 eV. The presence of the phenyl imide is confirmed by the reaction stoichiometry. Although the 2:1 aniline/oxygen ratio at low oxygen concentrations suggests an amide, with water being produced through steps 1 and 2 or step 3, the 1:1 the stoichiometry at high oxygen concentrations establishes the formation of a phenyl imide through step 4.

$$PhNH_2(g) + O(a) \rightarrow PhNH(a) + OH(a) \quad (1)$$

$$PhNH_2(g) + OH(a) \rightarrow PhNH(a) + H_2O(g) \quad (2)$$

$$2OH(a) \rightarrow O(a) + H_2O(g) \quad (3)$$

$$PhNH_2(g) + O(a) \rightarrow PhN(a) + H_2O(g) \quad (4)$$

These observations can be rationalized with a model in which step 4 is slow relative to (1) and (2) or (3) at low oxygen coverages but is dominant at high surface coverages, perhaps because of steric hindrance between the two aniline reactants or the need for two adjacent adsorption sites. The phenyl imide formed from (1) and/or (2) must be unstable at the surface with

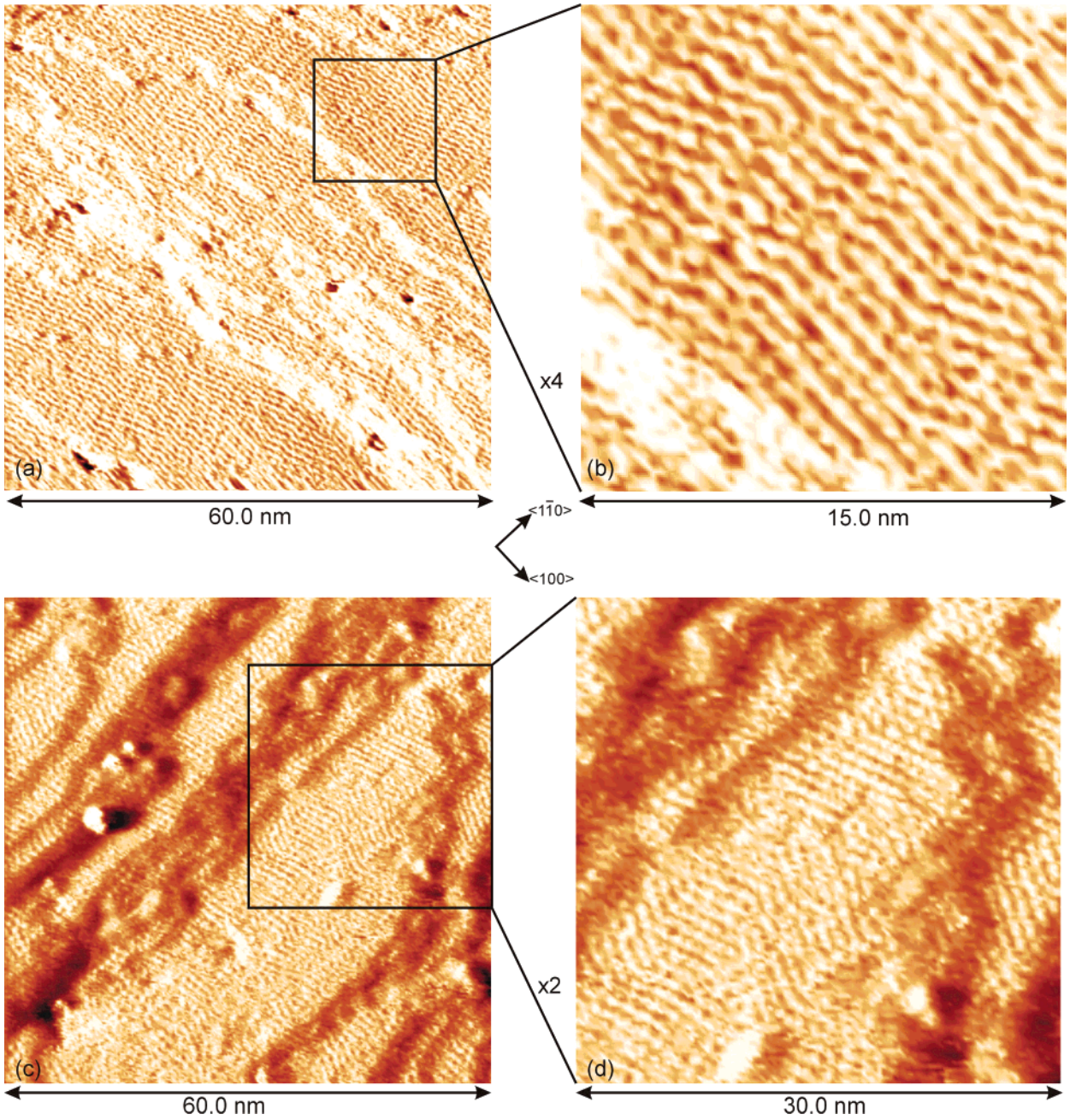

Figure 5. STM images showing the characteristic domain structure of a monolayer of phenyl imide generated by the reaction of aniline with preadsorbed oxygen at a Cu(110) surface at 293 K: (a and b) $V_S = 1.22$ V, $I_T = 3.05$ nA; (c and d) $V_S = 1.01$ V, $I_T = 2.42$ nA.

respect to the phenyl imide at 293 K, dissociating to give adsorbed hydrogen (step 5) which either remains at the surface or desorbs without further reaction with oxygen (step 6).

$$\mathrm{PhNH(a)} \rightarrow \mathrm{PhN(a)} + \mathrm{H(a)} \quad (5)$$

$$2\mathrm{H(a)} \rightarrow \mathrm{H_2(g)} \quad (6)$$

Similar stoichiometric changes have been observed[28] when ammonia reacts with chemisorbed oxygen suggesting a common mechanism; in that case, vibrational spectroscopy has shown that the product at room temperature is indeed the imide (NH(a)).

A detailed understanding of the reaction between ammonia and oxygen at copper surfaces has been developed in recent years. Where oxygen is preadsorbed, ammonia reacts with the ⟨100⟩ ends of the Cu−O chains[27,56] but if the oxygen transients that precede the chemisorbed islands can be intercepted (through low temperatures[57,58] or coadsorption at room temperature[28]) reaction is significantly faster and more selective. The nature and role of the oxygen transients has been discussed in detail elsewhere for a number of different systems,[23] but we emphasize here the extensive step movement that accompanies the coadsorption of aniline and dioxygen and the highly ordered adsorbate structure that results. These changes point to a very "flexible" surface during reaction. In addition, we note the high surface concentration of phenyl imide (3.4×10^{14} molecules cm^{-2}) that results from the coadsorption reaction. Assuming a square unit cell, this structure would have a *maximum* intermolecular spacing of 0.55 nm, the approximate van der Waals radius for the molecule is 0.6 nm.[59] In comparison, the equivalent imide (NH(a))[24] and phenoxy species[59] form c(2 × 4) and c(4 × 2) structures at Cu(110) surfaces respectively with

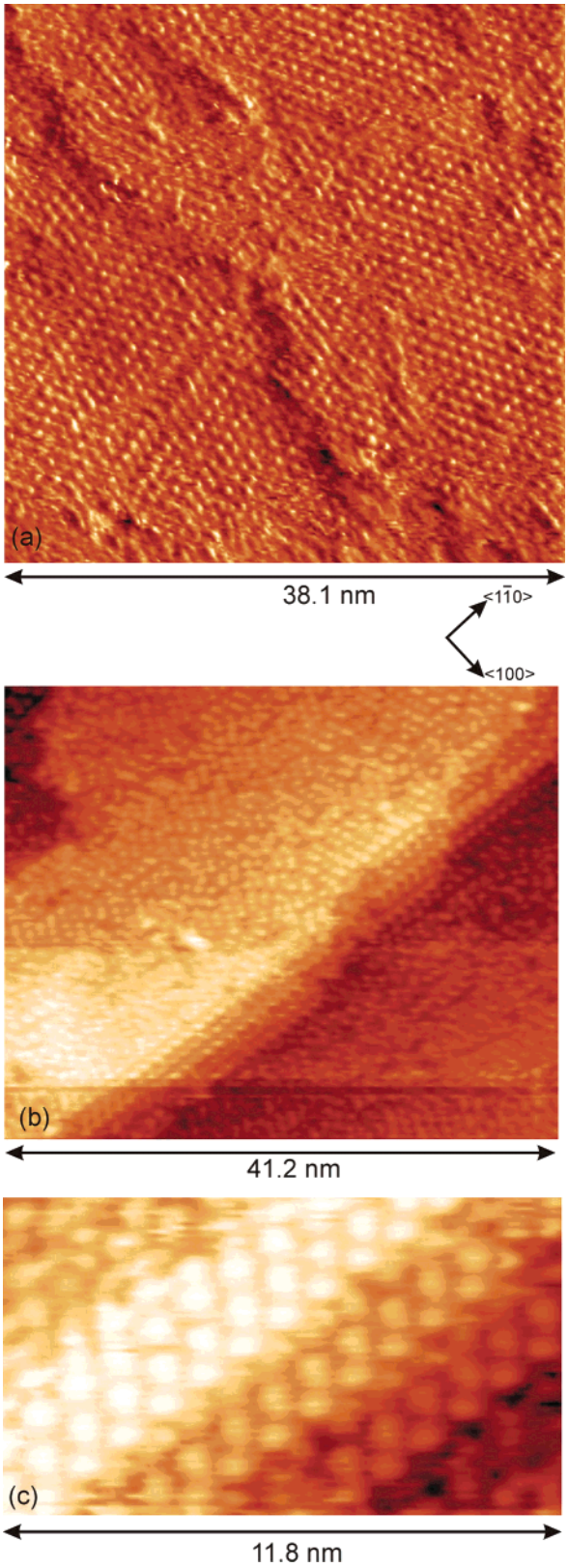

Figure 6. STM images showing atomically resolved domain structure of a monolayer of phenyl imide generated by the reaction of aniline with preadsorbed oxygen at a Cu(110) surface at 293 K: (a) $V_S = 1.22$ V, $I_T = 3.02$ nA; (b) $V_S = 1.26$ V, $I_T = 3.66$ nA; (c) close up of ordered imide structure at a step edge, $V_S = 1.27$ V; $I_T = 3.65$ nA.

maximum concentrations of 2.6×10^{14} molecules cm^{-2}. We return to this point in the discussion of the structures revealed by the STM images of the coadsorbed system below.

4.2. The Adsorption Site of the Imide. We consider next the adsorption site of the phenyl imide. From the size of the features imaged here and their similarity to those observed after adsorption of phenyl iodide at a Cu(110) surface, we conclude that it is the phenyl group that is imaged by STM. Figure 4b establishes that, in both the ⟨100⟩ and ⟨1$\bar{1}$0⟩ directions, these features are in line with the maxima in the oxygen lattice. The oxygen lattice consists of added copper−oxygen chains orientated in the ⟨100⟩ direction and STM images the copper rather than the oxygen atoms.[60] Furthermore, the added copper atoms are known to be situated in the hollow sites of the Cu(110) substrate. The extrapolation in Figure 4b therefore indicates that the phenyl rings are also located over a hollow site in the substrate lattice. This is in agreement with the adsorption sites identified for both phenyl species[53] and benzene[61] at Cu(110) surfaces. Interestingly, the favored adsorption site of NH(a) at Cu(110) surfaces is the short bridge site,[62,63] and as Figure 4e shows, if the phenyl imide is drawn using C−C and C−N bond lengths of 0.14 nm, typical values for aromatic molecules,[64] the nitrogen can be situated in the short bridge site with the phenyl ring situated above the hollow site.

Three ordered structures are observed when "high" coverages of the phenyl imide are obtained from reaction of aniline with chemisorbed oxygen, Figure 7, parts a−c. The structure in Figure 7a can be described with a centered rectangle unit cell with the long axis 1.4 nm in length in the ⟨100⟩ direction. This agrees well with a c(4 × 4) mesh (using Wood's notation) but for the present purposes a more useful description is the primitive unit cell given in matrix notation[55] by $\begin{pmatrix} 4 & 0 \\ 2 & 2 \end{pmatrix}$. The two other structures shown in Figure 7, parts b and c, are mirror images of each other about the ⟨100⟩ axis, with rhomboid unit cells ∼0.8 nm long at ±20° to the ⟨100⟩ axis; these correspond well with $\begin{pmatrix} 4 & 0 \\ -1 & 2 \end{pmatrix}$ and $\begin{pmatrix} 4 & 0 \\ 1 & 2 \end{pmatrix}$ unit meshes, respectively.

Models showing the relationship between the three structures are given in Figure 7d with the phenyl groups centered at the adsorption sites determined from Figure 4. Each has a spacing in the ⟨1$\bar{1}$0⟩ direction of 1.0 nm with the second "row" of phenyl imide two lattice spacings away in the ⟨100⟩ direction. The different structures are obtained by translating successive rows by ±1 or ±2 lattice positions in the ⟨1$\bar{1}$0⟩ direction. Interestingly, the p(4 × 2) structure, i.e. $\begin{pmatrix} 4 & 0 \\ 0 & 2 \end{pmatrix}$ in which successive rows of phenyl imide are aligned in the ⟨100⟩ direction, is not observed. Since this structure results in a smaller imide−imide nearest neighbor distance (0.72 nm) than the other three, its absence may indicate steric hindrance between adsorbed phenyl imides in the ⟨100⟩ direction. Although the exposure of the surface to aniline and dioxygen simultaneously results in a higher phenyl imide surface concentration, the minimum separation of the adsorbed molecules in the $\begin{pmatrix} 3 & 0 \\ 1 & 2 \end{pmatrix}$ structure remains greater than this value at 0.76 nm.

4.3. Adsorbate Ordering at the Cu(110) Surface. One of the most interesting observations from these experiments is the discrepancy between the coverages calculated from the STM images and the surface concentrations measured by XPS. If each feature in the STM images represents a phenyl imide then the three structures produced from reaction with preadsorbed oxygen have maximum surface coverages of $^1/_8$th of a monolayer, equivalent to a surface carbon concentration of 8.1×10^{14} cm^{-2}. The XPS data shows an actual carbon concentration of 16×10^{14} cm^{-2}. In the case of the coadsorption experiment, the

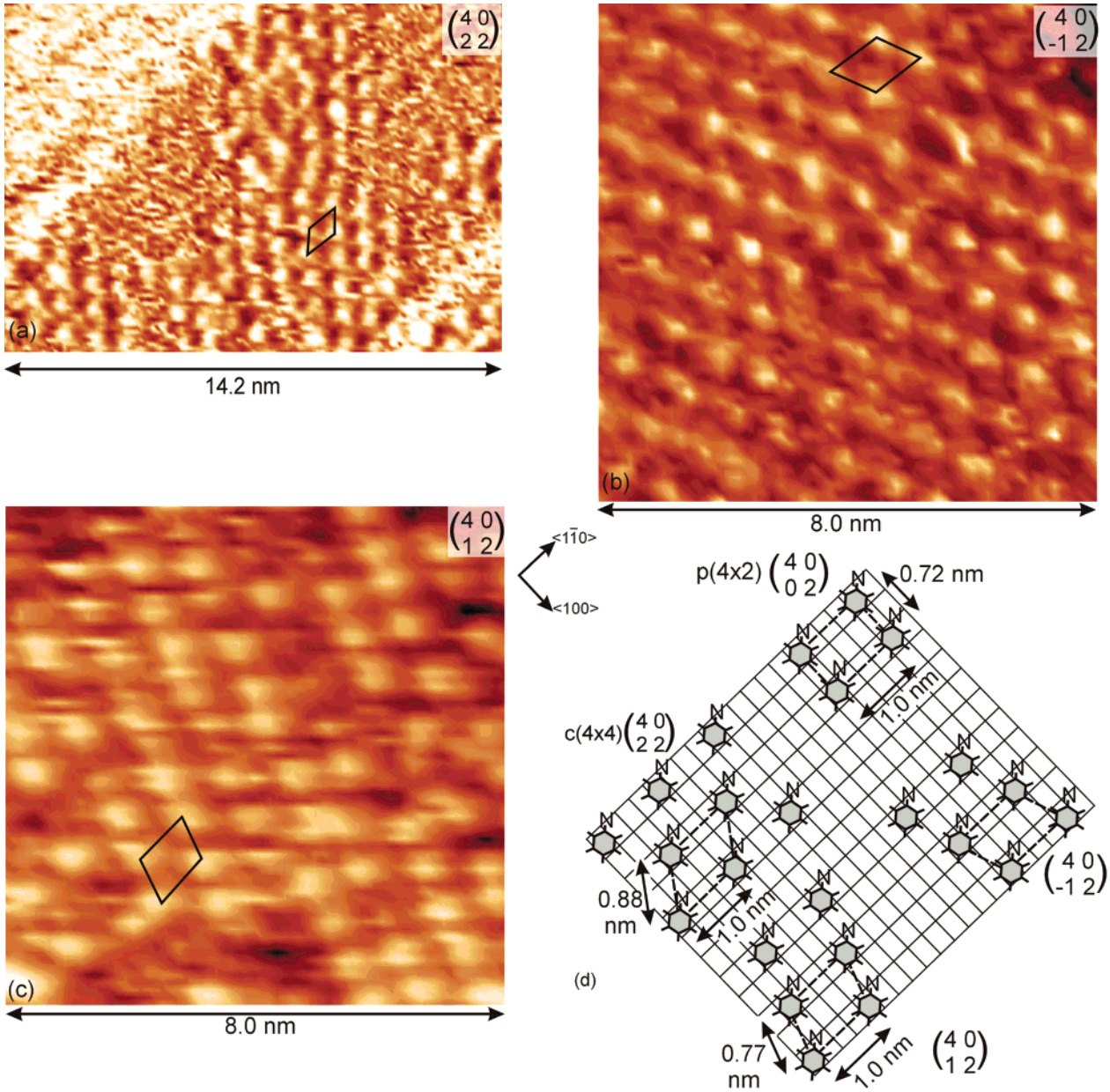

Figure 7. STM images of the three different domains present at a Cu(110) surface after the reaction of aniline with preadsorbed oxygen at 293 K: (a) $\begin{pmatrix} 4 & 0 \\ 2 & 2 \end{pmatrix}$, C(4 × 4) structure, $V_S = 0.80$ V, $I_T = 3.02$ nA; (b) $\begin{pmatrix} 4 & 0 \\ -1 & 2 \end{pmatrix}$, $V_S = 1.22$ V, $I_T = 3.07$ nA; (c) $\begin{pmatrix} 4 & 0 \\ 1 & 2 \end{pmatrix}$, $V_S = 1.22$ V, $I_T = 3.07$ nA. (d) Schematic showing possible structural models based on the adsorption site determined in Figure 4

$\begin{pmatrix} 3 & 0 \\ 1 & 2 \end{pmatrix}$ mesh has a maximum surface coverage of $^1/_6$th of a monolayer, equivalent to a carbon concentration of 1.1×10^{14} cm^{-2}. The XPS data shows an actual carbon concentration of 2.1×10^{14} cm^{-2}. We conclude that the unit cells shown by the STM contain two phenyl imide species.

Parts a and b of Figure 9 show two models which account for the high packing density and the "missing" phenyl groups in the STM images. Both models suggest strong aromatic interactions between the adsorbates. In Figure 9a, the phenyl rings are orientated in an edge-to-face T-shaped structure in which every other phenyl group is orientated perpendicular to the surface. Generally, phenyl rings bond parallel to metal surfaces, but the reduction in the heat of adsorption that results from the perpendicular orientation of half the rings could be compensated for by the formation of the T-shaped complex, which is known[65] to be a favorable structure for close packed aromatic systems. The alternative model, in Figure 9b, involves parallel phenyl pairs, a form of π-stacking, with the coordination of both nitrogens to the surface achieved by tilting the rings away from the surface plane. Parts c and d of Figure 9 show a possible model in which the lower phenyl ring is situated above a hollow site with the nitrogen atom in the short bridge site. The phenyl ring of the second molecule is parallel to the first, 0.15 nm above it and rotated by 65°, placing the nitrogen group above another short bridge site. By tilting the two phenyl rings at approximately 15° to the surface plane, around an axis which includes neither nitrogen atom, it is possible to bring the nitrogen of the upper ring to a similar height to that of the lower molecule. Surface vibrational spectroscopy has indicated that the phenyl ring is *close* to parallel to the surface,[47,66] but to date, these studies have concerned aniline reactions only with clean surfaces where the surface concentration of phenyl imide may not be high enough to force the formation of the π-stacked complex. Many other similar arrangements are possible for the

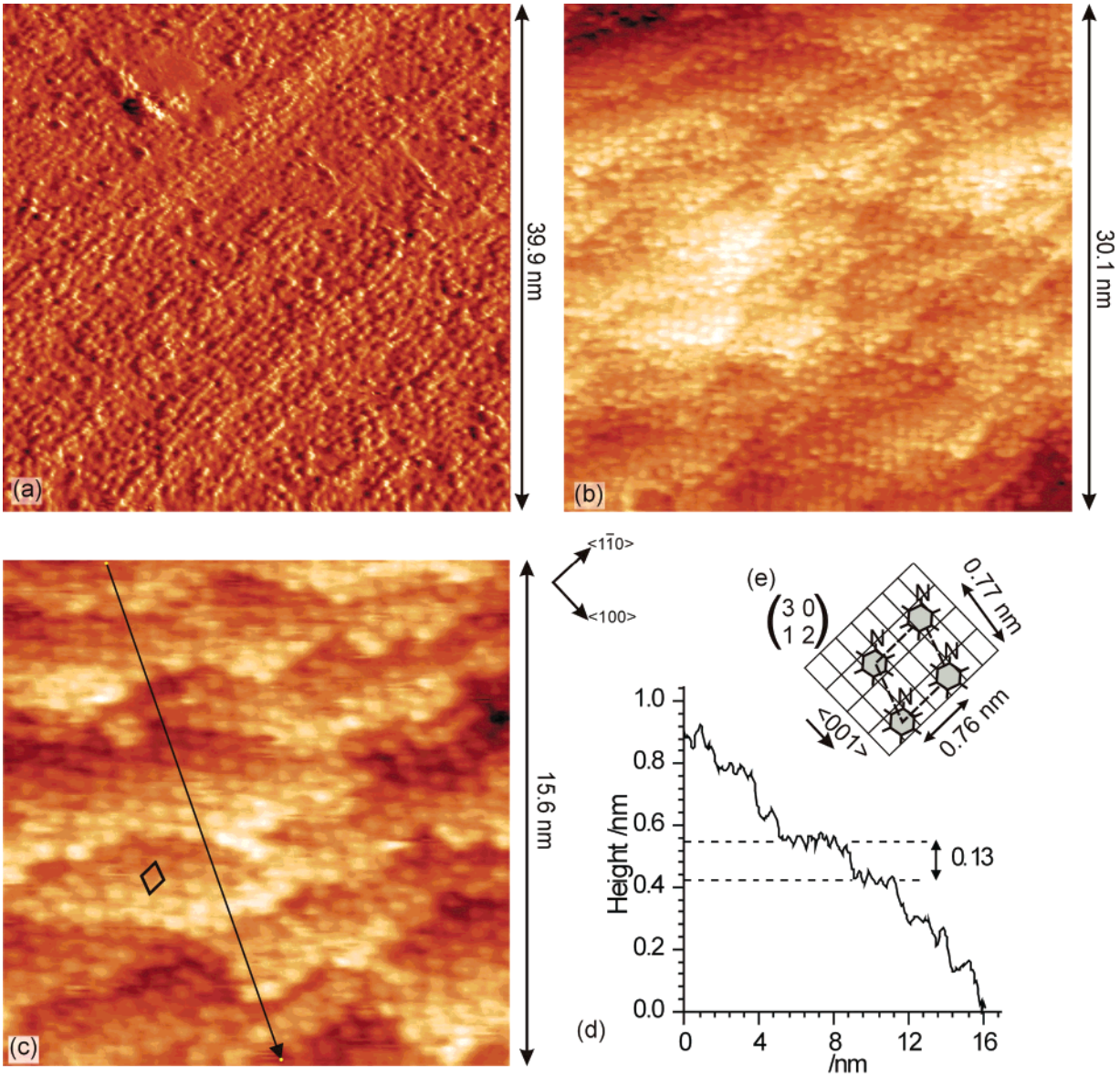

Figure 8. Comparison of STM images of high coverages of phenyl imide produced from (a) Cu(110) surface with an initial oxygen concentration of 2.4×10^{14} cm^{-2} exposed to 200 langmuir of aniline at 293 K, $V_S = 0.95$ V, $I_T = 1.93$ nA and (b) clean Cu(110) surface exposed to 200 langmuir of a 300:1 aniline/dioxygen mixture at 293 K, $V_S = 0.95$ V, $I_T = 2.04$ nA. (c) Close up of another area of the crystal after coadsorption, $V_S = 0.59$ V, $I_T = 2.89$ nA. (d) Line profile along line in part c showing short terraces and single atomic steps. (e) Model of the $\begin{pmatrix} 3 & 0 \\ 1 & 2 \end{pmatrix}$ structure using the adsorption site determined in Figure 4.

phenyl imide complex with the nitrogen atoms in different sites, but the model presented here has the advantage of a compact structure which would be consistent with the 0.7 nm diameter of the features observed in the STM images and also offers a explanation for the absence of the $\begin{pmatrix} 4 & 0 \\ 0 & 2 \end{pmatrix}$ and $\begin{pmatrix} 3 & 0 \\ 0 & 2 \end{pmatrix}$ structures from the surface, since these would result in the overlap of a nitrogen and a hydrogen at a bridge site, Figure 9f.

π-Stacking is associated with aromatic systems with reduced electron densities and differing polarizations, which conditions may be induced, in the present case by the interaction of the lower ring with the surface, the π-stacking interaction compensating for the reduced adsorption energy of the upper phenyl. π-Stacking of aromatic groups has been employed in the construction of 3-d supramolecular structures from large molecules such as porphyrins[67] and has been reported for smaller molecules deposited from solution[68,69] The present results, however, suggest that $\pi-\pi$ interactions play a significant role in the close packing of aromatic groups in a monolayer deposited from vacuum.

5. Conclusions

The reaction of aniline with surface oxygen has many characteristics in common with the equivalent reaction with ammonia, in particular, a similar dependence of the reaction stoichiometry on coverage suggesting similar reaction mechanisms, and a single imide product. The reaction with aniline is facile at room temperature, indicating that the weaker basicity of this molecule either does not affect the reaction or else is compensated for by the overall higher heat of adsorption of the phenyl ring and the weaker NH bond (335 ± 13 kJ mol^{-1} in aniline, 460 ± 8 kJ mol^{-1} in ammonia[70]). There was no indication of the formation of an intermediate structure involving an expanded (2×1)O(a) lattice as has been observed with pyridine and other amines.[32,50] By simultaneous imaging of the phenyl imide and the p(2×1)O(a) lattice, the phenyl group

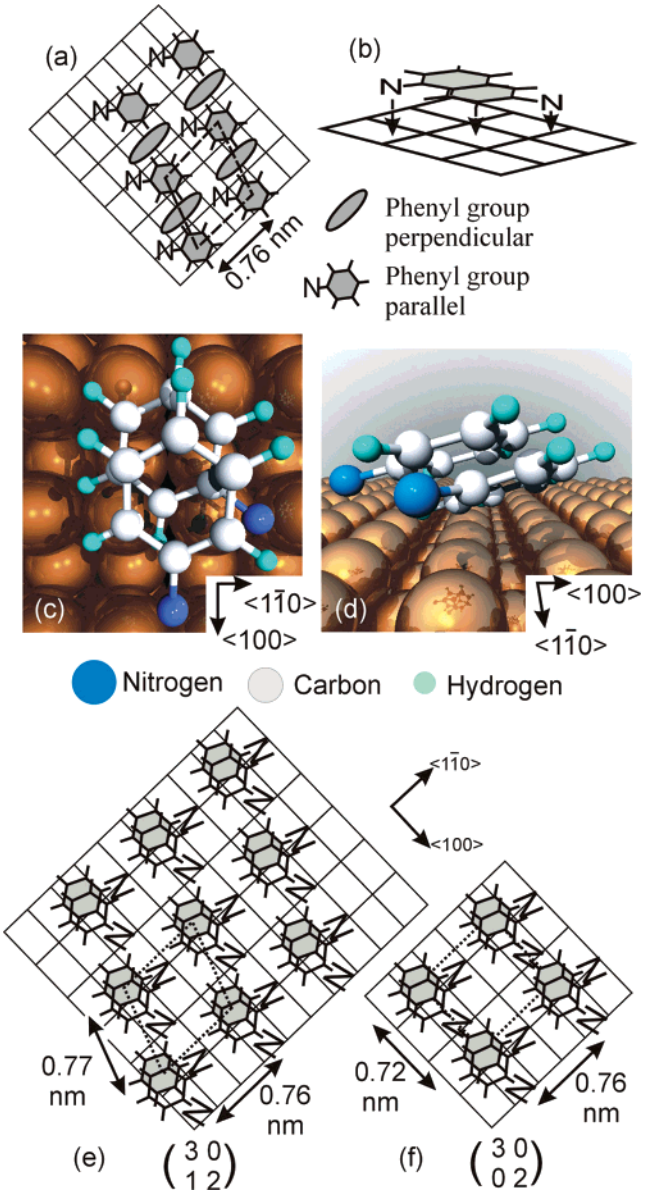

Figure 9. Models to account for the discrepancy between surface concentrations of phenyl imide calculated from STM and XP data: (a) edge-to-face, T-shaped packing of phenyl rings; (b) schematic of face-to-edge π-stacking model; (c) top and (d) side views of ball-and-stick drawing of the π-stacking model with phenyl rings tilted by 15° to surface plane; (e and f) models for the 2d structures of the phenyl imide dimers.

was shown to lie above the substrate hollow site, in this position the nitrogen atom of the imide can be placed over the short bridge site, the favored site for NH(a).

The maximum concentration of phenyl imide observed following exposure of *preadsorbed* oxygen to aniline was determined by XPS to be 2.6×10^{14} cm^{-2}. At this concentration the phenyl imide adlayer forms domains of three closely related ordered structures described by $\begin{pmatrix} 4 & 0 \\ 2 & 2 \end{pmatrix}$, $\begin{pmatrix} 4 & 0 \\ -1 & 2 \end{pmatrix}$, and $\begin{pmatrix} 4 & 0 \\ 1 & 2 \end{pmatrix}$ unit cells. Adsorption of aniline and dioxygen mixtures however leads to closer packing of the phenyl imides with a concentration calculated from the XPS spectra of 3.4×10^{14} cm^{-2} and an ordered adlayer described by $\begin{pmatrix} 3 & 0 \\ 1 & 2 \end{pmatrix}$ and $\begin{pmatrix} 3 & 0 \\ -1 & 2 \end{pmatrix}$ unit cells.

The surface concentrations calculated from the XPS for the ordered phenyl imide structures are twice that calculated from the unit cells revealed by the STM. Furthermore, the high phenyl imide concentrations indicate a nearest neighbor distance that is less than the van der Waals radius of the molecule. To account for these observations it is proposed that attractive $\pi-\pi$ interactions between the phenyl imide adsorbates give rise to π-stacking in the monolayer.

Acknowledgment. This work was supported by EPSRC and The Royal Society.

References and Notes

(1) Lazarova, E.; Petkova, G.; Raicheff, R.; Neykov, G. *J. Appl. Electrochem.* **2002**, *32*, 1355.
(2) Khaled, K. F.; Hackerman, N. *Electrochim. Acta* **2004**, *49*, 485.
(3) Du, T. B.; Chen, J. J.; Cao, D. Z. *J. Mater. Sci.* **2001**, *36*, 3903.
(4) Luo, H.; Guan, Y. C.; Han, K. N. *Corrosion* **1998**, *54*, 721.
(5) Khaled, K. F.; Hackerman, N. *Mater. Chem. Phys.* **2003**, *82*, 949.
(6) Gaillard, F.; Joly, J. P.; Peillex, E.; Romand, M. *J. Adhes.* **2000**, *72*, 317.
(7) Li, Z. F.; Ruckenstein, E. *J. Colloid Interface Sci.* **2002**, *251*, 343.
(8) Harun, M. K.; Lyon, S. B.; Marsh, J. *Prog. Org. Coat.* **2003**, *46*, 21.
(9) Johnsen, B. B.; Olafsen, K.; Stori, A. *Int. J. Adhes. Adhes.* **2003**, *23*, 157.
(10) Marsh, J.; Minel, L.; Barthes-Labrousse, M. G.; Gorse, D. *Appl. Surf. Sci.* **1998**, *133*, 270.
(11) Penzien, J. C.; Haessner, C.; Jentys, A.; Kohler, K.; Muller, T. E.; Lercher, J. A. *J. Catal.* **2004**, *221*, 302.
(12) Bronnimann, C.; Bodnar, Z.; Aeschimann, R.; Mallat, T.; Baiker, A. *J. Catal.* **1996**, *161*, 720.
(13) Huntsman, W. D.; Madison, N. L.; Schlesinger, S. I. *J. Catal.* **1963**, *2*, 498.
(14) Struijk, J.; Scholten, J. J. F. *Appl. Catal., A* **1992**, *82*, 277.
(15) Pfaltz, A.; Heinz, T. *Top. Catal.* **1997**, *4*, 229.
(16) Wells, P. B.; Wilkinson, A. G. *Top. Catal.* **1998**, *5*, 39.
(17) Bartok, M.; Felfoldi, K.; Szollosi, G.; Bartok, T. *Catal. Lett.* **1999**, *61*, 1.
(18) Bartok, M.; Felfoldi, K.; Torok, B.; Bartok, T. *Chem. Commun.* **1998**, 2605.
(19) Torok, B.; Felfoldi, K.; Szakonyi, G.; Balazsik, K.; Bartok, M. *Catal. Lett.* **1998**, *52*, 81.
(20) Tungler, A.; Mathe, T.; Tarnai, T.; Fodor, K.; Toth, G.; Kajtar, J.; Kolossvary, I.; Herenyi, B.; Sheldon, R. A. *Tetrahedron: Asym.* **1995**, *6*, 2395.
(21) Davies, P. R.; Keel, J. M. *Catal. Lett.* **1999**, *58*, 99.
(22) Davies, P. R.; Keel, J. M. *Surf. Sci.* **2000**, *469*, 204.
(23) Carley, A. F.; Davies, P. R.; Roberts, M. W. *Catal. Lett.* **2002**, *80*, 25.
(24) Carley, A. F.; Davies, P. R.; Jones, R. V.; Harikumar, K. R.; Kulkarni, G. U.; Roberts, M. W. *Top. Catal.* **2000**, *11*, 299.
(25) Carley, A. F.; Davies, P. R.; Roberts, M. W. *Chem. Commun.* **1998**, 1793.
(26) Carley, A. F.; Davies, P. R.; Roberts, M. W.; Thomas, K. K.; Yan, S. *Chem. Commun.* **1998**, 35.
(27) Carley, A. F.; Davies, P. R.; Roberts, M. W.; Vincent, D. *Top. Catal.* **1994**, *1*, 35.
(28) Afsin, B.; Davies, P. R.; Pashusky, A.; Roberts, M. W.; Vincent, D. *Surf. Sci.* **1993**, *284*, 109.
(29) Afsin, B.; Davies, P. R.; Pashuski, A.; Roberts, M. W. *Surf. Sci.* **1991**, *259*, L724.
(30) Carley, A. F.; Davies, P. R.; Harikumar, K. R.; Jones, R. V.; Kulkarni, G. U.; Roberts, M. W. *Top. Catal.* **2001**, *14*, 101.
(31) Carley, A. F.; Yan, S.; Roberts, M. W. *J. Chem. Soc., Faraday Trans.* **1990**, *86*, 2701.
(32) Carley, A. F.; Davies, P. R.; Jones, R. V.; Kulkarni, G. U.; Roberts, M. W. *Chem. Commun.* **1999**, 687.
(33) Davies, P. R.; Shukla, N. *Surf. Sci.* **1995**, *322*, 8.
(34) Thornburg, D. M.; Madix, R. J. *Surf. Sci.* **1990**, *226*, 61.
(35) Sasaki, T.; Aruga, T.; Kuroda, H.; Iwasawa, Y. *Surf. Sci.* **1992**, *276*, 69.
(36) Maseri, F.; Peremans, A.; Darville, J.; Gilles, J. M. *J. Electron Spectrosc. Relat. Phenom.* **1990**, *54*, 1059.
(37) Sasaki, T.; Aruga, T.; Kuroda, H.; Iwasawa, Y. *Surf. Sci.* **1991**, *249*, L347.
(38) Gardin, D. E.; Somorjai, G. A. *J. Phys. Chem.* **1992**, *96*, 9424.
(39) Erley, W.; Hemminger, J. C. *Surf. Sci.* **1994**, *316*, L1025.
(40) Erley, W.; Xu, R.; Hemminger, J. C. *Surf. Sci.* **1997**, *389*, 272.
(41) Chen, J. J.; Winograd, N. *Surf. Sci.* **1995**, *326*, 285.
(42) Birtill, J. J.; Ridley, P.; Liddle, S.; Nunney, T. S.; Raval, R. *Ind. Eng. Chem. Res.* **2001**, *40*, 553.
(43) Barlow, S. M.; Haq, S.; Raval, R. *Langmuir* **2001**, *17*, 3292.

(44) Xu, X. P.; Friend, C. M. *J. Vac. Sci. Technol. A—Vac. Surf. Films* **1991**, *9*, 1599.
(45) Bitzer, T.; Alkunshalie, T.; Richardson, N. V. *Surf. Sci.* **1996**, *368*, 202.
(46) Rummel, R. M.; Ziegler, C. *Surf. Sci.* **1998**, *418*, 303.
(47) Ashton, M. R.; Jones, T. S.; Richardson, N. V.; Mack, R. G.; Unertl, W. N. *J. Electron Spectrosc. Relat. Phenom.* **1990**, *54*, 1133.
(48) Carley, A. F.; Roberts, M. W. *Proc. R. Soc. London, Ser. A* **1978**, *363*, 403.
(49) Carley, A. F.; Davies, P. R.; Jones, R. V.; Harikumar, K. R.; Kulkarni, G. U.; Roberts, M. W. *Surf. Sci.* **2000**, *447*, 39.
(50) Carley, A. F.; Davies, P. R.; Edwards, D.; Parsons, M.; Roberts, M. W. Manuscript in preparation.
(51) Cabibil, H.; Ihm, H.; White, J. M. *Surf. Sci.* **2000**, *447*, 91.
(52) Carley, A. F.; Coughlin, M.; Davies, P. R.; Morgan, D. J.; Roberts, M. W. *Surf. Sci. Lett.* **2004**, in press.
(53) Carley, A. F.; Coughlin, M.; Davies, P. R.; Morgan, D. J.; Roberts, M. W. *Surf. Sci.* **2004**, *555*, L138.
(54) Weiss, P. S.; Kamna, M. M.; Graham, T. M.; Stranick, S. J. **1998**, *14*, 1284.
(55) Park, R. L.; Madden, H. H., Jr. *Surf. Sci.* **1968**, *11*, 188.
(56) Guo, X. C.; Madix, R. J. *Faraday Discuss.* **1996**, 139.
(57) Carley, A. F.; Davies, P. R.; Kulkarni, G. U.; Roberts, M. W. *Catal. Lett.* **1999**, *58*, 93.
(58) Sueyoshi, T.; Sasaki, T.; Iwasawa, Y. *J. Phys. Chem.* **1996**, *100*, 1048.
(59) Guo, X. C.; Madix, R. J. *Surf. Sci.* **1995**, *341*, L1065.
(60) Buisset, J.; Rust, H. P.; Schweizer, E. K.; Cramer, L.; Bradshaw, A. M. *Surf. Sci.* **1996**, *349*, L147.
(61) Rogers, B. L.; Shapter, J. G.; Ford, M. *Surf. Sci.* **2004**, *548*, 29.
(62) Davies, P. R.; Keel, J. M. *Phys. Chem. Chem. Phys.* **1999**, *1*, 1383.
(63) Hirschmugl, C. J.; Schindler, K. M.; Schaff, O.; Fernandez, V.; Theobald, A.; Hofmann, P.; Bradshaw, A. M.; Davis, R.; Booth, N. A.; Woodruff, D. P.; Fritzsche, V. *Surf. Sci.* **1996**, *352*, 232.
(64) Walker, B. W.; Stair, P. C. *Surf. Sci.* **1981**, *103*, 315.
(65) Hunter, C. A.; Lawson, K. R.; Perkins, J.; Urch, C. J. *J. Chem. Soc., Perkin Trans. 2* **2001**, 651.
(66) Plank, R. V.; Dinardo, N. J.; Vohs, J. M. *Surf. Sci.* **1995**, *340*, L971.
(67) Gesquiere, A.; De Feyter, S.; De Schryver, F. C.; Schoonbeek, F.; van Esch, J.; Kellogg, R. M.; Feringa, B. L. *Nano Lett.* **2001**, *1*, 201.
(68) Pinheiro, L. S.; Temperini, M. L. A. *Surf. Sci.* **1999**, *441*, 45.
(69) Pinheiro, L. S.; Temperini, M. L. A. *Surf. Sci.* **2000**, *464*, 176.
(70) *CRC Handbook of Chemistry and Physics*; 59th ed.; Weast, R. C., Ed.; CRC Press Inc: Boca Raton, FL, 1979; pp F215.